ISSN 0027-1349, Moscow University Physics Bulletin, 2017, Vol. 72, No. 3, pp. 287–293. © Allerton Press, Inc., 2017.
Original Russian Text © A.V. Kuznetsov, N.V. Klenov, 2017, published in Vestnik Moskovskogo Universiteta, Seriya 3: Fizika, Astronomiya, 2017, No. 3, pp. 69–75.

CONDENSED MATTER PHYSICS

# An Optimization Method for the Calculation of Hamiltonian Matrix Elements for Josephson Flux Qubits

**A. V. Kuznetsov[a]* and N. V. Klenov[a, b, c]****

[a] *Department of Physics, Moscow State University, Moscow, 119991 Russia*
[b] *Moscow Technological Institute (MIREA), pr. Vernadskogo 78, Moscow, 119454 Russia*
[c] *Moscow Technical University of Communications and Informatics, Moscow, 111024 Russia*
**e-mail: kuznetsov-1992@mail.ru*
***e-mail: nvklenov@gmail.com*

Received July 11, 2016; in final form, July 28, 2016

**Abstract**—This work aims to describe the method of analytical calculation of an orthonormalized basis of states of the Josephson flux quantum bits (qubits) using a two-level approximation under the condition that the potential energy of the system is a combination of two potential wells separated by a tunnel barrier. For illustration, the calculation results in the case of the well-known three- and four-junction flux qubits, as well as promising silent qubits, are presented.

**Keywords:** flux qubits, Hamiltoniam matrix, spin basis, Bloch equation, silent qubits.

**DOI:** 10.3103/S0027134917030080

## INTRODUCTION

The development of modern solid-state electronics follows the path of constant reduction of the characteristic size of the working element of the logical cell in information processing. The analysis of the dynamics of quantum systems, including the spins of single electrons in solids [1], as well as atomic [2] and superconducting [3] quantum bits (qubits), is increasingly relevant. Superconducting qubits with micrometer dimensions [4] that allow the effective control of separate "artificial atoms" are considered in this article.

During modeling and optimization of any characteristics of quantum mechanical systems, an essential part of the computational power is spent on searching for the spectrum and matrix elements of the Hamiltonian of the quantum system. In addition, a detailed study of the dynamics of superconducting qubits cannot be imagined without an analysis of the loss of coherence of qubit states. In particular, the coherence loss time, normalized to the duration of the characteristic processes in the system, determines the maximum number of the logical operations produced by a logical element [5]. There are different ways of describing the processes of coherence loss in qubit systems [6, 7], but in the simplest case, the dissipative dynamics of the two-level superconducting Josephson's qubit in the presence of control magnetic flux is described by the Bloch equation for the density matrix of the system [8, 9]. In this equation the Hamiltonian is defined in the form of the matrix $\hat{H}(t) = \begin{pmatrix} H_{11} & H_{12} \\ H_{21} & H_{22} \end{pmatrix}$, $H_{ij}(t) = \langle \phi_i(t)|\hat{H}(t)|\phi_j(t)\rangle$, $i,j = 1,2$ in an orthonormalized basis of the wave functions $\phi_1(x_1 \ldots x_n, t)$ and $\phi_2(x_1 \ldots x_n, t)$, with $x_1, \ldots, x_n$ being the set of generalized coordinates of the system. The main part of this paper aims specifically at calculating the matrix elements of the Hamiltonian for various qubit systems. The proposed method for a rapid search for the basis wave functions and the Hamiltonian matrix of a two-level system will provide a dramatic acceleration of calculation of any characteristics of superconducting flux qubits on the basis of the Bloch equation. This approach to the calculation of the matrix elements of the Hamiltonian will be used to analyze three- and four-junction flux qubits (Figs. 1a, 1b), as well as silent qubits (Fig. 1c).

In addition, we note that the Josephson qubit control field can be defined in either an oscillatory or a unipolar form. The first method has been well studied [10]. For unipolar fields, there is reason to believe on the basis of the simplified models [11–13] that they can also be used for optimal control of the qubit systems, including the picosecond time scale. Therefore, in this paper, in analyzing the dynamics of qubit systems, a unipolar control field will be used. In addition, we will attempt to show that these results can be used to study the effect of ultrashort unipolar pulses of the control field on the qubit.

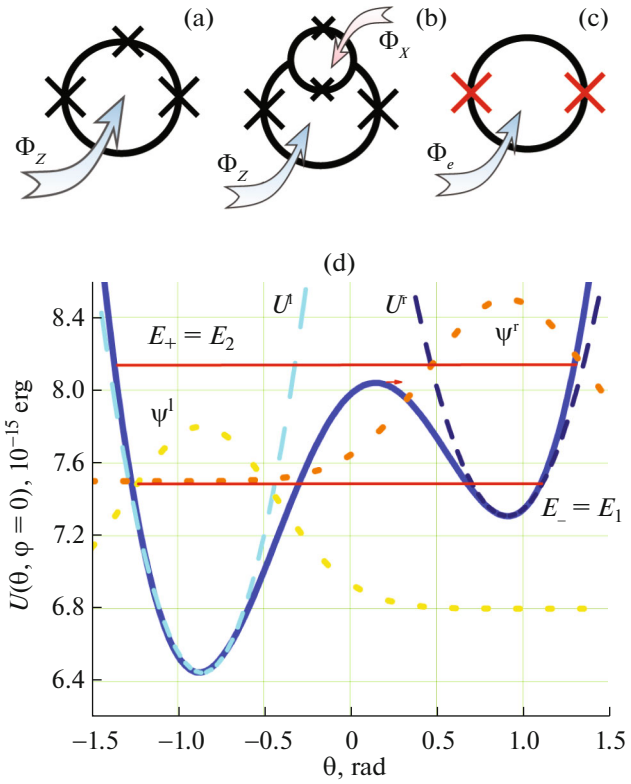


**Fig. 1.** A schematic view of a three-junction flux qubit (a); four-junction flux qubit (b); silent qubit (c). The crosses on the schemes denote the Josephson junctions with critical currents $I_C$; $\alpha I_C$ and capacitances $C$; $\alpha C$; $\varphi_1$, $\varphi_2$, $\varphi_3$, $\varphi_4$ are the phases of the Josephson junctions; $\Phi_Z$, $\Phi_X$, $\Phi_e$ are the magnetic fluxes. (d) A typical graph of the potential energy of a flux qubit and its approximations with the potential functions of the harmonic oscillator. As an example, the section of the potential energy of the 3JJ qubit by the plane $\varphi = 0$ is shown near the point of degeneracy at $f_z = 0.0175$, $\alpha = 0.8$, $E_J = 5 \times 10^{-15}$ erg, as well as the approximating functions $U^l(\theta, \varphi)$, $U^r(\theta, \varphi)$ (dash curves) and the wave functions of the stationary states in these potentials, $\psi^l(\theta, \varphi)$ and $\psi^r(\theta, \varphi)$ (dot curves).

## 1. METHOD FOR THE CALCULATION OF THE HAMILTONIAN MATRIX OF THE JOSEPHSON QUBIT

It is well known [14] that a Josephson qubit can be described well under certain conditions by a two-level model system in which the wave function has the form

$$\psi(x_1 \ldots x_n, t) = c_1(t)\phi_1(x_1 \ldots x_n, t) + c_2(t)\phi_2(x_1 \ldots x_n, t). \quad (1)$$

In this case, the normalization condition is fulfilled: $|c_1(t)|^2 + |c_2(t)|^2 = 1$. The possibility of using a two-level model significantly simplifies the analysis of the functioning of the qubit [15, 16], allowing us to immediately write the expression for the eigenvalues of the Hamiltonian of a two-level system:

$$E_\pm = \bar{E} \pm \sqrt{\Delta^2 + V^2}, \quad \bar{E} = \frac{H_{11} + H_{22}}{2}, \quad \Delta = \frac{H_{22} - H_{11}}{2}, \quad V = H_{12}. \quad (2)$$

The application of (2) for analyzing the dynamics of qubits on the basis of the quantum-mechanical equation $i\hbar \frac{d}{dt}\begin{pmatrix} c_1(t) \\ c_2(t) \end{pmatrix} = \begin{pmatrix} H_{11} & H_{12} \\ H_{21} & H_{22} \end{pmatrix}\begin{pmatrix} c_1(t) \\ c_2(t) \end{pmatrix}$ provides rather high accuracy if the system changes occur in a quasi-stationary mode:

$$\Xi(t) = \left| \left( \frac{\partial E_\pm}{\partial t} \right) / \frac{E_\pm}{T} \right|_{\mathrm{MAX}\forall t>0} \ll 1. \quad (3)$$

In the process of calculation of the qubit dynamics, the fulfillment of this condition was controlled by the simplest numerical assessment of the time derivatives of the eigenvalues of energy ($\Xi(t) \le 0.04$).

Determination of the spin basis and general approaches to express the Lagrange function in the context of the quantum-mechanical analogy for flux qubits are described in the Appendix. We formulate here the most important simplification of the proposed method: the potential energy profile $U(x_1, \ldots, x_n)$ with two minima (a double-well potential) allows one to use the approximation by the potential energy profile of the linear harmonic oscillator (Fig. 1d). The approximating functions have the form

$$\begin{cases} U^l(x_1, \ldots, x_n, t) = U_0^l + \sum_{k=1}^{n} \frac{M_{x_k}}{2} (\omega_{x_k}^l)^2 (x_k - (x_k)_{\min}^l)^2 \\ U^r x_1, \ldots, x_n, t) = U_0^r + \sum_{k=1}^{n} \frac{M_{x_k}}{2} (\omega_{x_k}^r)^2 (x_k - (x_k)_{\min}^r)^2. \end{cases} \quad (4)$$

The basis function $\psi^l(x_1, \ldots, x_n, t)$ of the spin basis corresponds to the left minimum (l), the basis function $\psi^r(x_1 \ldots x_n, t)$ corresponds to the right minimum (r). The first stage of the described method is to find expressions for generalized masses $M_{x_1}, \ldots, M_{x_n}$. We emphasize that the final result of the paper will be obtained when considering the qubits described by the potential energy $U(x_1, \ldots, x_n)$ without any simplification of this function. However, before this, one should carry out an auxiliary consideration to determine the wave functions of the spin basis of the system. In this treatment, we temporarily ignore the coordinate domains $(x_1, \ldots, x_n)$, which correspond to the potential barrier between the minima $U(x_1, \ldots, x_n)$ and/or contain points far from each minimum. The potential energy function itself is temporarily replaced by one of functions (4) with index $l$ or $r$, depending on what minimum is considered. After having found the wave functions, all further analysis will be valid for all possible values of coordinates $x_1$–$x_n$ for the exact (not approximate) form of the potential energy. The very problem of finding the spin basis reduces to the well-known problem of the linear harmonic oscillator [17] (detailed calculations are given in the Appendix).

At the second stage, we represent the potential energy in a certain domain in the form of (4) and

determine the expressions for characteristic frequencies $\omega_{x_1}^{r/l}$, $\omega_{x_n}^{r/l}$, "sizes" $a_{x_1}^{r/l}$, $a_{x_n}^{r/l}$ and dimensionless coordinates $\xi_{x_1}^{r/l}$, $\xi_{x_n}^{r/l}$. As a result, the functions of spin basis normalized to unity will also be determined. To perform the orthogonalization procedure, we write the basis functions in the form

$$\phi_{l,2}(x_1, ..., x_n, t) = \frac{\psi^{l/r}(x_1, ..., x_n, t) + c(\psi^l(x_1, ..., x_n, t) + \psi^r(x_1, ..., x_n, t))}{\sqrt{1-(\psi^l\psi^r)}}. \quad (5)$$

Here, $c = \frac{1}{2}\left(-1 + \sqrt{\frac{1-(\psi^l\psi^r)}{1+(\psi^l\psi^r)}}\right)$. All calculations below were first performed in the basis $\{\psi^l, \psi^r\}$ and further they were recalculated into basis (5).

The third stage of the implementation of the proposed method is the same for all qubits under consideration. This reduces to the calculation of the terms of the Hamiltonian matrix elements that correspond to the kinetic energy. The kinetic energy operator has the same form for each of the two minima:

$$\hat{T} = -\sum_{k=1}^{n} \frac{\hbar^2}{2M_{x_k}} \frac{\partial^2}{\partial(x_k)^2} = -\sum_{k=1}^{n} \frac{\hbar\omega_{x_k}^{r/l}}{2} \frac{\partial^2}{\partial(\xi_{x_k}^{r/l})^2}. \quad (6)$$

For matrix elements $H_{11}$, $H_{22}$ and $H_{12} = H_{21}$, the terms that correspond to the kinetic energy are calculated by the formulas obtained in the Appendix:

$$\begin{cases} \tilde{T}_{11} = \sum_{k=1}^{n} \frac{\hbar\omega_{x_k}^{l}}{4}; \quad \tilde{T}_{22} = \sum_{k=1}^{n} \frac{\hbar\omega_{x_k}^{r}}{4}; \\ \tilde{T}_{12} = \tilde{T}_{21} = D2^{\frac{n}{2}-1} \sum_{k=1}^{n} \frac{\hbar\omega_{x_k}^{r}}{c_{x_k}^2+1}(c_{x_k}^2 - z_{0x_k}^2). \end{cases} \quad (7)$$

For correct calculation, we should pass to basis (5):

$$\begin{cases} T_{11} = (\tilde{T}_{11}(1+c)^2 + 2c(c+1)\tilde{T}_{12} + c^2\tilde{T}_{22})/(1-(\psi^l\psi^r)) \\ T_{22} = (\tilde{T}_{22}(1+c)^2 + 2c(c+1)\tilde{T}_{12} + c^2\tilde{T}_{11})/(1-(\psi^l\psi^r)) \\ T_{12} = T_{21} = (\tilde{T}_{12}(2c^2+2c+1) + (\tilde{T}_{11}+\tilde{T}_{22})(c^2+c))/(1-(\psi^l\psi^r)). \end{cases} \quad (8)$$

The fourth stage of the calculation of the Hamiltonian matrix reduces to the integration of the product of a pair of basis functions by the potential energy of the system, which is now taken not in an approximate form of the linear harmonic oscillator, but in its original form for this system. The auxiliary expressions that are necessary for the integration of the potential energy are given in the Appendix.

Thus, we summarize the steps for calculating the Hamiltonian matrix of a qubit system with a potential energy that has two minima.

The Lagrange function of the system is written using the expressions for the functions $M_{x_1}, ..., M_{x_n}$.

The potential energy of the system near the points of minima is represented in form (4), and expressions for the characteristic frequencies, sizes and dimensionless coordinates must be obtained.

Formulas (7) and (8) must be used to calculate the kinetic energy term.

For each pair of the basis wave functions $\{\psi^l, \psi^r\}$ the potential energy integral of the system is calculated between the brackets of a pair of these basis functions and then one should pass to basis (5) using formulas (8) and replacing $T$ by $V$.

Now, let us consider specific qubit systems.

## 2. A THREE- OR FOUR-JUNCTION FLUX QUBIT

We consider a three-junction flux qubit (abbreviated as 3JJ qubit) [3, 18], which is a well-known system on the basis of Josephson's junctions [19]. It is described by two variables, $\theta$ and $\varphi$ ($n = 2$). The 3JJ qubit (Fig. 1a) consists of Josephson's junctions 1, 2, 3, included in a superconducting circuit with the magnetic flux $\Phi_z$ penetrating it. Junctions 1 and 2 are the same and have a definite area, critical current $I_C$, capacitance $C$, and the Josephson energy $E_J = \hbar I_C/(2e)$, whereas for junction 3 these parameters are less by $\alpha = (E_J)_3/(E_J)_1 \in [0.5;1]$ times. For a four-junction (4JJ) qubit shown in Fig. 1b, the role of the Josephson junction no. 3 is played by a two-junction interferometer with the penetrating external magnetic flux $\Phi_x$. It is possible to control the parameter $\alpha$ in the 4JJ qubit via the external magnetic flux $\Phi_x$, whereas parameter $\alpha$ is a constant in the 3JJ qubit. In particular, if both junctions of a small superconducting circuit of the system in Fig. 1b are identical and have parameters $I_C/2$, $C/2$, and $E_J/2$, then $\alpha = \cos(\pi\Phi_x/\Phi_0)$. Since the condition $\alpha > 1/2$ must be satisfied for the double-well potential to exist, one should also provide the validity of the condition $|\pi\Phi_x/\Phi_0| < \arccos(1/2)$. For other characteristics, the dynamics of these devices is analogous, since a two-contact interferometer is equivalent to an isolated Josephson junction with the phase $\varphi_{eff} = (\varphi_3 + \varphi_4)/2$.

In this Section all phases are counted clockwise both in large ($\Phi_z$) and small ($\Phi_x$) superconducting circuits. Below, all results obtained for the 3JJ qubit will take place for the 4JJ qubit, although this is not specifically stipulated for brevity. For the 4JJ qubit, one should also use two variables, namely $\theta \equiv x_1$ and $\varphi \equiv x_2$, $n = 2$. When comparing 3JJ and 4JJ qubits, we must take the formulas into account for $\alpha$ and $\varphi_{\text{eff}}$ ($\varphi_{\text{eff}}$ is the effective phase of a small superconducting ring of the 4JJ qubit; hereinafter, it is designated as $\varphi_3$ if the 4JJ qubit is meant).

Below we will assume that the inductance of all superconducting circuits is sufficiently small: $LI_C \ll \Phi_0$, $\Phi_0 = \dfrac{h}{2e}$ is the quantum of magnetic flux. Only in this case the magnetic flux that penetrates the circuits approximately equals the externally given magnetic flux $\Phi_z$ (or $\Phi_x$). For brevity, we will use the designation $f_z = \Phi_z/\Phi_0 - 1/2$; the point $f_z = 0$ is called the point of degeneracy and corresponds to the case when the potential energy shown in Fig. 1d has a symmetric form. At $|f_z| > (f_z)_{\text{crit}}$, $(f_z)_{\text{crit}} \sim 0.1$ one minimum of the potential energy of the qubit disappears. We will consider only those values of $f_z$ that do not strongly differ from zero.

As known from the Josephson effect theory [20, 21], the current through the junction is related to the phase $\varphi$. The assessments of the critical current $I_C$ and energy $E_J$ are: ~400 nA and ~ $10^{-15}$ erg, respectively [4]. When the junctions in a superconducting ring are connected in series, their phases are added and the total Josephson's phase is rigidly connected with the magnetic flux penetrating the ring [22]. Due to this one obtains

$$\varphi_1 + \varphi_2 + \varphi_3 = 2\pi(f_z + 1/2). \tag{9}$$

By performing the transformations (see Appendix for more details) with allowance for the formulas and designations $M = (\hbar/2e)^2 C$, $M_\theta = 2M(1 + 2\alpha)$, $M_\varphi = 2M$, $s = E_J/E_C$, $E_C = (2e)^2/(2C)$, we obtain the quantities $U_0^{r/l}$, $\omega_\theta^{r/l}$, and $\omega_\varphi^{r/l}$. The potential part of the Hamiltonian takes the form

$$\begin{cases} \tilde{V}_{11} = E_J\left(2 + \alpha - \dfrac{1}{2}\cos\theta_{\min}^{l}\tilde{f}(a_\theta^{l})\tilde{f}(a_\varphi^{l}) + \dfrac{\alpha}{2}\cos z^{l}\tilde{f}(2a_\theta^{l})\right), \\ \tilde{V}_{22} = E_J\left(2 + \alpha - \dfrac{1}{2}\cos\theta_{\min}^{r}\tilde{f}(a_\theta^{r})\tilde{f}(a_\varphi^{r}) + \dfrac{\alpha}{2}\cos z^{r}\tilde{f}(2a_\theta^{r})\right), \\ \tilde{V}_{12} = E_J D\left(4 + 2\alpha - \cos z_2\tilde{f}(z_1)\tilde{f}(z_3) + \alpha\cos z_5\tilde{f}(z_4)\right). \end{cases} \tag{10}$$

The kinetic energy is calculated by formulas (7) and (8). Parameters (10) should be also substituted into (8) with replacing $T$ by $V$. We now compare our results to the results of other authors. It should be emphasized that to date, even the distance between the basis levels of the qubit was not found theoretically with sufficient accuracy. When compared with the experiment, the "energy gap" $E_2 - E_1$ is usually treated as an adjustable parameter [3]. Unlike this, we expressed this quantity analytically through the Hamiltonian matrix. Its adequacy can be verified by comparing it with the results of numerical simulation. Analytical calculations are reduced to the use of the above formulas obtained in the Appendix. The numerical calculations were based on the direct calculation of the integrals for the matrix elements of the kinetic and potential energy $\tilde{T}_{ij}, \tilde{V}_{ij}$, $i, j = 1,2$ using the two-dimensional method of rectangles.

The energies of the stationary states of a three-junction flux qubit depending on the parameters $f_z$ and $\alpha$ are shown in Figs. 2a and 2b. Figure 2a demonstrates complete correspondence to the literature data [3, 23, 24] shown in Fig. 2c, while Fig. 2b is in partial agreement with the data [23] (Fig. 2d) for all values of $\alpha$ except the region near $\alpha \approx 0.5$. This is due to the fact that, unlike our consideration, the calculations in [23] were carried out with allowance for the presence of no less than four energy levels of flux qubit. The analysis of the simplest logical operations on such a system is presented in the Appendix.

## 3. SILENT QUBITS

A silent qubit is a two-junction interferometer controlled by the magnetic flux. It contains two Josephson's junctions with the non-trivial current-phase dependence (CFD)

$$I_S(\varphi) = A\sin\varphi - B\sin(2\varphi), \quad A > 0, \quad B > A/2 > 0. \tag{11}$$

These qubits are treated as a promising modification of the flux qubits regarding the possibility of minimizing the intensity of uncontrolled interaction with the environment [25–30]. In addition, the standard working value of the magnetic flux for silent qubits is $|\varphi_e| \ll 1$, $\varphi_e \equiv 2\pi\Phi_e/\Phi_0$, in particular $\varphi_e = 0$. This is much more convenient than in the case of the 3JJ qubits (Fig. 2a), when the external flux should be equal to $\Phi_0/2$, and the smallest detuning from this value changes the distance between the energy levels

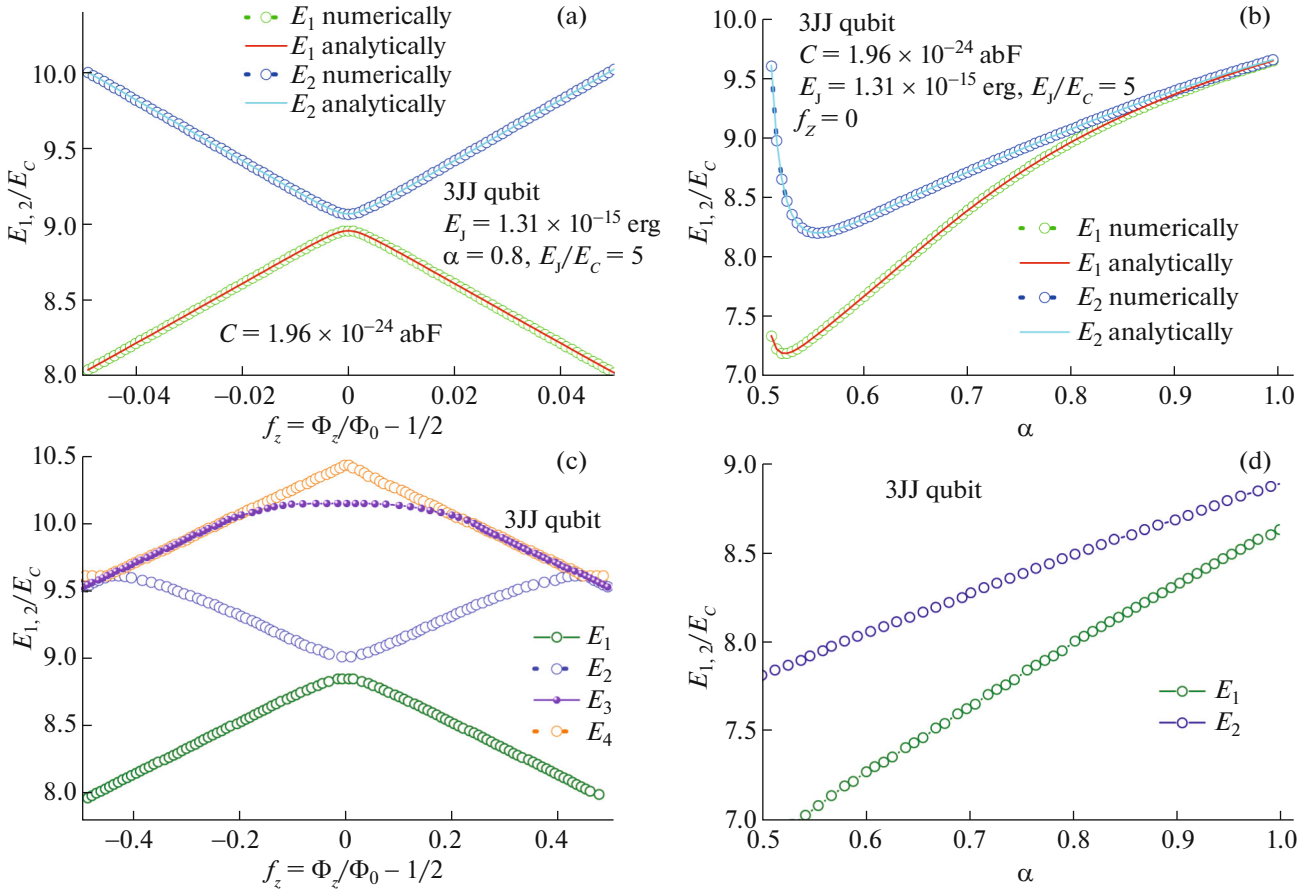


**Fig. 2.** The energy dependencies of the stationary states of the 3JJ qubit as functions of $f_z$ at $\alpha = 0.8$ (a) and $\alpha$ at $f_z = 0$ (b) at $E_J = 1.31 \times 10^{-15}$ erg, $E_J/E_C = 5$, $C = 1.96 \times 10^{-24}$ abF; for comparison, we show the dependencies of the first energy levels on the external flux $f_z$ at $\alpha = 0.8$ (c) and parameter $\alpha$ at $f_z = 0$ (d), according to [23].

by an order of magnitude. Below, we will assume that the inductance of the interferometer is negligible ($|2\pi LA/\Phi_0| \ll 1$).

For a silent qubit, in the formulas of Section 1 we must use the value $n = 1$ and a single variable $\theta \equiv x_1$ (this variable has the different meaning compared to the variable $\theta$ for the 3JJ and 4JJ qubits). Let the directions of counting of the Josephson phases for junctions 1 and 2 be chosen so that $\varphi_e = \varphi_1 - \varphi_2$; therefore $\varphi_2 = \varphi_1 - \varphi_e$, and the potential energy is given by the coordinate $\theta \equiv \varphi_1$, $O \equiv \{(\theta): \theta \in (-\infty, \infty)\}$. Then, assuming that the total current through the junction is $(I_{\text{sum}})_j = (I_S)_j + \frac{\hbar}{2e} C_j \ddot{\varphi}_j$, $j = 1,2$, using the first Kirchhoff law $(I_{\text{sum}})_1 = (I_{\text{sum}})_2$, the condition $|\ddot{\varphi}_e| \ll |\ddot{\varphi}_{1,2}|$, notations

$$\begin{cases} E_{A1} = \dfrac{\hbar A_1}{2e}, \quad E_{B1} = \dfrac{\hbar B_1}{2e}, \quad E_{A2} = \dfrac{\hbar A_2}{2e}, \quad E_{B2} = \dfrac{\hbar B_2}{2e}, \quad M_\theta = M_1 + M_2 \\ E_A = E_{A1} + E_{A2}, \quad E_B = E_{B1} + E_{B2}, \quad M_1 = \left(\dfrac{\hbar}{2e}\right)^2 C_1, \quad M_2 = \left(\dfrac{\hbar}{2e}\right)^2 C_2, \end{cases} \tag{12}$$

and integrating Eq. (11) over the phase for junctions 1 and 2, the potential energy takes the form

$$U(\theta) = -E_{A1}\cos\theta + (E_{B1}/2)\cos 2\theta - E_{A2}\cos(\theta - \varphi_e) + (E_{B2}/2)\cos(2\theta - 2\varphi_e). \tag{13}$$

A detailed derivation of the expressions for the constants that are needed to find the matrix elements of the Hamiltonian is given in the Appendix. The kinetic energy is calculated by substituting them into (7) and (8), and the oscillator frequency and the potential energy have the form

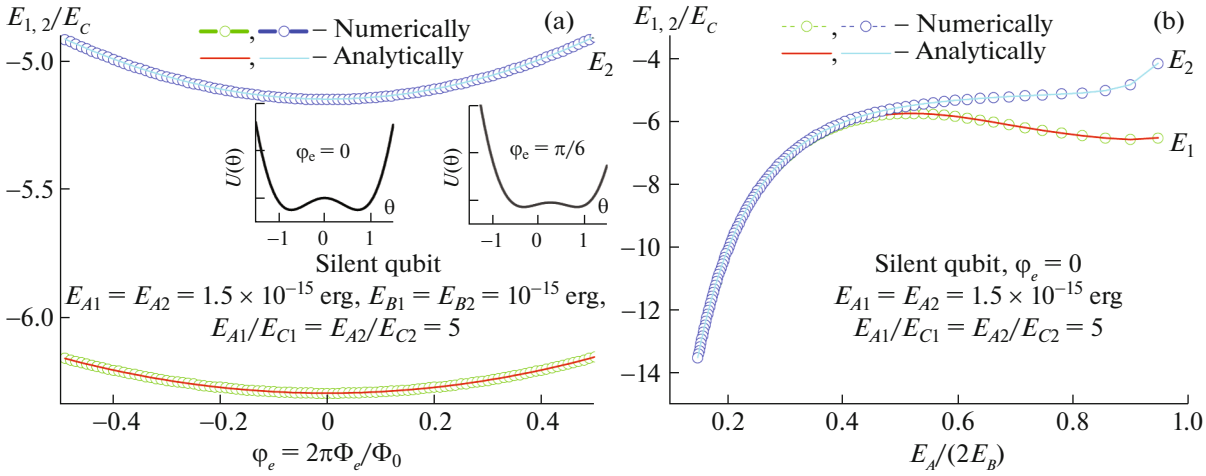


**Fig. 3.** Energies $E_1 \equiv E_-$ and $E_2 \equiv E_+$ of the stationary states of a symmetrical silent qubit as functions of the external magnetic flux $\varphi_e$ ($E_{B1} = E_{B2} = 10^{-15}$ erg) (a) and parameter $E_A/(2E_B)$ ($\varphi_e = 0$) (b) at $E_{A1} = E_{A2} = 1.5 \times 10^{-15}$ erg and $E_{A1}/E_{C1} = E_{A2}/E_{C2} = 5$.

$$\omega_\theta^{r/l} = \left\{\left(\frac{4E_B^2 - E_A^2}{2E_B} + \frac{\varphi_e((E_A/E_B)^2 + 2)}{\sqrt{4E_B^2 - E_A^2}}(E_{A2}E_{B1} - E_{A1}E_{B2})\right)/M_\theta\right\}^{\frac{1}{2}}, \tag{14}$$

$$\begin{aligned}\tilde{V}_{12} = \tilde{V}_{21} = &-\frac{D}{\sqrt{2}}(E_{A1}\cos z_2 + E_{A2}\cos(z_2 - \varphi_e))\tilde{f}(z_1)\\ &+\frac{D}{2\sqrt{2}}(E_{B1}\cos 2z_2 + E_{B2}\cos(2z_2 - 2\varphi_e))\tilde{f}(2z_1),\end{aligned} \tag{15}$$

$$\begin{aligned}\tilde{V}_{11/22} = \frac{1}{2}\Bigg\{&\tilde{f}(a_\theta^{l/r})(-E_{A1}\cos\theta_{\min}^{l/r} - E_{A2}\cos(\theta_{\min}^{l/r} - \varphi_e))\\ &+\tilde{f}(2a_\theta^{l/r})\left(\frac{E_{B1}}{2}\cos 2\theta_{\min}^{l/r} + \frac{E_{B2}}{2}\cos(2\theta_{\min}^{l/r} - 2\varphi_e)\right)\Bigg\}.\end{aligned} \tag{16}$$

Expressions (15) and (16) should be substituted into (8) replacing $T$ by $V$ (in (8)).

To illustrate the results, we study the energies of the stationary states of a symmetric silent qubit $E_1 \equiv E_-$, $E_2 \equiv E_+$ as functions of the applied flux $\varphi_e$ and the weight of the first harmonic $E_A/(2E_B)$. Figure 3a shows their dependence on the relative external magnetic flux penetrating the circuit. One can see from the figure that the dependence of $E_2 - E_1$ from $\varphi_e$ is much less manifested than in the case of the 3JJ qubit. Moreover, in a symmetrical silent qubit, the function $U(\theta)$ preserves the symmetry for different values of $\varphi_e$, which is shown in the insets to Fig. 3a. The opposite situation takes place in the case of the 3JJ qubit, in which the magnetic flux $f_z$ controls the potential energy asymmetry. It can be shown that in an asymmetric silent qubit the function $U(\theta)$ ceases to be symmetric for $\varphi_e \neq 0$, as in the 3JJ qubit for $f_z \neq 0$. In this case the dependence $E_1 \equiv E_-$ and $E_2 \equiv E_+$ on $\varphi_e$ does not qualitatively differ from the one considered above.

The dependence of the stationary states energies of a silent qubit on the parameter $E_A/(2E_B)$ in the case of a symmetric qubit (Fig. 3b) shows that the energy difference $E_1 \equiv E_-$ and $E_2 \equiv E_+$ rapidly tends to zero with decreasing parameter $E_A/(2E_B)$. This can be easily explained qualitatively, since as the value of $\theta_0^{r/l} = \pm\arccos(E_A/(2E_B))$ increases the distance between the right and left minima of the potential energy $U(\theta)$ increases. Due to this, the intensity of tunneling between the minima of the potential energy becomes small. Thus, $H_{12}$ and $H_{21}$ tend to zero, and the difference $H_{11} - H_{22}$ exactly equals zero due to the symmetry of $U(\theta)$. By (2), this leads to closeness of the energies of the first and second stationary states of the system.

## CONCLUSIONS

A calculation method has been proposed that makes it possible to find the spin and energy basis and the Hamiltonian matrix elements of the flux qubit analytically. We considered the examples of three-junction, four-junction, and silent qubits and demonstrated the possibility of using the described procedure in definite ranges of values of the control magnetic flux of the system at small (compared to the Josephson's frequency of the system) rates of its variation that do not violate the condition of quasistationarity.

The dependence of the energy gap of qubits on the amplitude of the magnetic flux measured from the degeneracy point and on the relationships of the Josephson energies of the system transitions has been investigated both analytically and numerically. It is shown that for a silent qubit the dependence of the energy gap on the flux is much less expressed than for three-junction and four-junction flux qubits. This can be useful for optimal control of the parameters of the qubit systems. As well, the energy gap in flux qubits strongly depends on the distance between the minima of the double-well potential.

## ACKNOWLEDGMENTS

The work was supported by the grant of the President of Russia, project no. 5813.2016.2 (Sections 1 and 2), and the Russian Foundation for Basic Research, no. 16-29-09515_ofi_m (Section 3). The authors are thankful to M.V. Denisenko for presenting the data and useful discussions.

## REFERENCES

1. D. D. Awschalom, L. C. Bassett, A. S. Dzurak, et al., Science **339**, 1174 (2013). doi 10.1126/science.1231364
2. J. J. Pla, K. Y. Tan, J. P. Dehollain, et al., Nature **489**, 541 (2012). doi 10.1038/nature11449
3. A. N. Omel'yanchuk, E. V. Il'ichev, and S. N. Shevchenko, *Quantum Coherent Phenomena in Josephson Qubits* (Naukova Dumka, Kyiv, 2013).
4. https://www.royalholloway.ac.uk/physics/documents/pdf/research/fluxqubit.pdf.
5. M. H. Devoret and R. J. Schoelkopf, Science **339**, 1169 (2013). doi 10.1126/science.1231930
6. https://aqpl.mc2.chalmers.se/~gojo71/KvantInfo/Decoherence_Bloch_Equations.pdf.
7. N. V. Klenov, A. V. Sharafiev, S. V. Bakurskiy, and V. K. Kornev, IEEE Trans. Appl. Supercond. **21**, 864 (2011). . doi 10.1109/TASC.2010.2093490
8. M. O. Scully and M. S. Zubairy, *Quantum Optics* (Cambridge Univ. Press, 1997).
9. H.-P. Breuer and F. Petruccione, *The Theory of Open Quantum Systems* (Oxford Univ. Press, 2002).
10. J. Q. You and F. Nori, Nature **474**, 589 (2011). doi 10.1038/nature10122
11. N. V. Klenov, A. V. Kuznetsov, I. I. Soloviev, et al., Beilstein J. Nanotechnol. **6**, 1946 (2015). doi 10.3762/bjnano.6.199
12. I. I. Soloviev, N. V. Klenov, A. L. Pankratov, et al., Phys. Rev. B **92**, 014516 (2015). doi 10.1103/PhysRevB.92.014516
13. I. I. Soloviev, N. V. Klenov, S. V. Bakurskiy, et al., Appl. Phys. Lett. **105**, 202602 (2014). doi 10.1063/1.4902327
14. A. J. Leggett, S. Chacravarty, A. T. Dorsey, et al., Rev. Mod. Phys. **59**, 1 (1987).
15. https://ocw.mit.edu/courses/electrical-engineering-and-computer-science/6-728-applied-quantum-and-statistical-physics-fall-2006/study-materials/twolevel04.pdf.
16. L. D. Landau and E. M. Lifshitz, *Quantum Mechanics: Non-Relativistic Theory* (Nauka, Moscow, 1989).
17. I. Askerzade, Low Temp. Phys. **41**, 241 (2015). doi 10.1063/1.4916071
18. E. V. Il'ichev and Ya. S. Grinberg, *Quantum Informatics and Quantum Bits Based on Superconducting Josephson Structures* (Novosib. Gos. Tekh. Univ., Novosibirsk, 2013).
19. A. Barone and G. Paterno, *Physics and Applications of the Josephson Effect* (Wiley, New York, 1982).
20. B. D. Josephson, Phys. Lett. **1**, 251 (1962). doi 10.1016/0031-9163(62)91369-0
21. B. D. Josephson, Rev. Mod. Phys. **36**, 216 (1964). doi 10.1103/RevModPhys.36.216
22. K. K. Likharev and B. T. Ul'rikh, *Systems with Josephson Contacts. Theoretical Framework* (Mosk. Gos. Univ., Moscow, 1978).
23. M. V. Denisenko, Candidate's Dissertation in Mathematics and Physics (Lobachevsky State Univ. of Nizhny Novgorod, Nizhny Novgorod, 2016).
24. I. Chiorescu, Y. Nakamura, C. J. P. M. Harmans, and J. E. Mooij, Science **299**, 1869 (2003). doi 10.1126/science.1081045
25. E. Goldobin, H. Sickinger, M. Weides, et al., Appl. Phys. Lett. **102**, 242602 (2013). doi 10.1063/4811752
26. S. V. Bakurskiy, N. V. Klenov, T. Yu. Karminskaya, et al., Supercond. Sci. Technol. **26**, 015005 (2013). doi 10.1088/0953-2048/26/1/015005
27. N. V. Klenov, N. G. Pugach, A. V. Sharafiev, S. V. Bakurskiy, and V. K. Kornev, Phys. Solid State **52**, 2246 (2010). doi 10.1134/S1063783410110053
28. N. Klenov, V. Kornev, A. Vedyayev, et al., J. Phys.: Conf. Ser. **97**, 012037 (2008). doi 10.1088/1742-6596/97/1/012037
29. N. Klenov, V. Kornev, and N. Pedersen, Phys. C **435**, 114 (2006). doi 10.1016/j.physc.2006.01.027
30. M. H. S. Amin, A. Yu. Smirnov, A. M. Zagoskin, et al., Phys. Rev. B **71**, 064516 (2005). doi 10.1103/PhysRevB.71.064516

*Translated by G. Dedkov*